Molecular Crystals and Liquid Crystals Science and Technology. Section A. Molecular Crystals and Liquid Crystals

Publication details, including instructions for authors and subscription information:
http://www.tandfonline.com/loi/gmcl19

Photogeneration of Solitons and Polarons in MX Chains

Hiroshi Okamoto [a] , Yasuo Oka [a] , Tadaoki Mitani [b] , Koshiro Toriumi [c] & Masahiro Yamashita [d]

[a] Research Institute for Scientific Measurements, Tohoku Univ., Katahira, Sendai, 980, Japan

[b] Japan Advanced Institute of Science and Technology, Hokuriku, Ishikawa, 923-12, Japan

[c] Department of Material Science, Himeji Institute of Technology, Hyogo, 678-12, Japan

[d] Graduate School of Human Informatics, Nagoya Univ., Nagoya, 464-01, Japan

Version of record first published: 04 Oct 2006.

To cite this article: Hiroshi Okamoto , Yasuo Oka , Tadaoki Mitani , Koshiro Toriumi & Masahiro Yamashita (1994): Photogeneration of Solitons and Polarons in MX Chains, Molecular Crystals and Liquid Crystals Science and Technology. Section A. Molecular Crystals and Liquid Crystals, 256:1, 161-170

To link to this article: http://dx.doi.org/10.1080/10587259408039244

Mol. Cryst. Liq. Cryst. 1994, Vol. 256, pp. 161–170
Reprints available directly from the publisher
Photocopying permitted by license only

PHOTOGENERATION OF SOLITONS AND POLARONS IN MX CHAINS

HIROSHI OKAMOTO and YASUO OKA
Research Institute for Scientific Measurements, Tohoku Univ., Katahira, Sendai 980, Japan.
TADAOKI MITANI
Japan Advanced Institute of Science and Technology, Hokuriku, Ishikawa 923–12, Japan
KOSHIRO TORIUMI
Department of Material Science, Himeji Institute of Technology, Hyogo 678–12, Japan
MASAHIRO YAMASHITA
Graduate School of Human Informatics, Nagoya Univ., Nagoya 464–01, Japan

Abstract The effects of the electron–lattice (e–l) coupling and the interchain interaction on the gap states in the one–dimensional Peierls–Hubbard system have been investigated by the photo–induced absorption (PA) measurements of the halogen–bridged metal complexes (the MX chains; M=Pt and X=Cl, Br or I).

In the complexes having small amplitude of CDW, three PA bands named $\mathbf{a}_1$, $\mathbf{a}_2$ and **b** are observed. The PA bands $\mathbf{a}_1$ and $\mathbf{a}_2$, which are insensitive to the interchain interaction, are assigned to polarons. The decrease of the interchain coupling of CDW leads to a midgap band **b**, which is attributable to charged–solitons. While, in the complexes having large amplitude of CDW, there are observed the two PA bands **A** and **B** having the long life time. Spectral shapes and excitation profiles of these PA bands are considerably different from those of the $\mathbf{a}_1$, $\mathbf{a}_2$ and **b** bands. These results suggest that generation processes and stabilization energies of the gap states are strongly dependent on the magnitude of e–l interactions.

INTRODUCTION

Topological solitons in the one–dimensional (1–D) system with lattice instability, has been attracting much attention after the pioneering work on polyacetylene.[1] It has been experimentally revealed that the concepts of soliton and other nonlinear excitations are essential for understanding the optical and magnetic properties as well as the transport properties of the 1–D system.[2] Subsequently, the halogen(X)–bridged metal(M) complexes (or equivalently the MX chain compounds) expressed as $[\cdots M^{3-\rho}\cdots X^{-}\!\!-\!\!M^{3+\rho}X^{-}\cdots M^{3-\rho}\cdots X^{-}\!\!-\!\!M^{3+\rho}X^{-}\cdots]$ ($0\leq\rho<1$) have provided a unique opportunity to study the instability of the 1–D Peierls–Hubbard system, because of the remarkable tunability of the electronic states.

In the MX compounds, the displacement of the bridging halogen, that is, the amplitude of the charge–density–wave (CDW) state can be controlled by the replacements of the metal (M=Pt, Pd, Ni) and the bridging halogen (X=Cl, Br, I) constituting the 1–D chains, and the ligand molecule and the counter anion surrounding them.[3,4] In the complexes having large halogen distortions, an electron–hole pair in a chain is strongly localized by the effect of electron–lattice (e–l) interac–

tion, where the self-trapping of the charge-transfer (CT) exciton and the large stokes shift of the luminescence have been observed. On the other hand, with decrease of the halogen distortions, the 1-D electronic states become delocarized. It is expected in this case that the dynamical behaviors of the low-lying nonlinear excitations, namely the gap states such as solitons and polarons, dominate the optical and transport properties. In fact, in the complexes having small halogen distortions, intensity of luminescence is considerably decreased and the photo-current is enhanced, suggesting that efficiency of dissociation of the photo-excited electron-hole pair increases.[3] In addition to the amplitude of CDW, the dimensionality of CDW, i.e. the phase correlation between the 1-D CDW states can be modified by changing the strength of the inter-chain hydrogen(H)-bonds.[3,4] Such a control of the CDW states allows us to make an advanced study of dynamics of the gap states.

In this paper, first, the chemical modifications to control the CDW states are reported. After that, the results of the photo-induced absorption (PA) measurements on the MX compounds are presented, where the spectral shapes, time-characteristics, and excitation profiles of the PA signals have been systematically investigated, concentrating our attention on the amplitude and interchain interaction of CDW. The PA spectra of the complexes having small halogen distortions are composed of the three PA bands named $\mathbf{a}_1$, $\mathbf{a}_2$ and **b**. By taking into account the effect of the interchain interaction on the gap states, the two bands ($\mathbf{a}_1$ and $\mathbf{a}_2$) are assigned to polarons, and the mid-gap band (**b**) to charged-solitons. The spectral characteristics of the PA signals can be directly compared with theoretical calculations[5-8] based on the 1-D Peierls-Hubbard model. While, in the complexes having large halogen distortions, another type of PA bands with relatively long life time has been observed in common, which are so-called **A** and **B** bands.[9] By comparing the spectral shapes and excitation profiles of these PA bands ($\mathbf{a}_1$, $\mathbf{a}_2$, **b** and **A**, **B**), the effects of e-l interaction on the gap states will be discussed in detail.

EXPERIMENTAL

The PA measurements in the IR and visible regions were made by using an FTIR spectrometer (Nicolet system 800) equipped with an InSb or an MCT detector and a 25cm monochromator (Jasco CT-25) with a PbS cell or a photomultiplier, respectively. As an excitation light, Ar-laser (5145A) was used. For measurements of the excitation-spectra of the PA signals, a 650W halogen-tungsten lamp or a 75W Xe lamp monochromized by a f=10 cm monochromator (Jasco CT-10) was utilized. The experimental procedures to obtain PA spectra ($-\Delta T/T$: the photo-induced change of the transmittance spectra T) have been reported elsewhere in detail.[10] The single crystals used were synthesized in the same way as reported in Ref.3.

CONTROL OF THE CDW STATES

The halogen-bridged metal complexes are represented as $[M^{3-\rho}A_2][M^{3+\rho}A_2X_2]Y_4$ ($0 \leq \rho < 1$) (or simply $\{MA_2X\}Y_2$), where A and Y are the ligand molecule and the counter anion, respectively.

In these complexes, the $[MA_2]$ moieties are bridged by the halogen ions (X), and the H–bonds between the amino–groups of the ligands (A) and the counter anions (Y) support the MX chains, as schematically illustrated in Figure 1. The 1–D electronic state is composed of $d_z{}^2$ orbitals of metals and p_z orbitals of bridging halogens. In the Pt or Pd complexes, the mono–valence state $[-M^{3+}-X^{-}-M^{3+}-X^{-}-M^{3+}-X^{-}-M^{3+}-X^{-}-]$ is unstable due to the e–l interaction and stabilized into the mixed–valence (CDW) state $[\cdot\cdot M^{3-\rho}\cdot\cdot X^{-}-M^{3+\rho}X^{-}\cdot\cdot\cdot M^{3-\rho}\cdot\cdot X^{-}-M^{3+\rho}X^{-}\cdot\cdot]$.

By replacing the metal (M=Pt, Pd or Ni) and the bridging–halogen ion (X=Cl, Br or I), the Coulomb repulsion energy (U) on the metal site and the transfer energy (T) between the nearest neighbor metal sites are considerably changed, respectively, since the sizes of the orbitals are different among the respective metals (M) and halogen ions (X). Thus, it is expected to obtain a variety of complexes having different structural parameters; e.g. the valency of the metals $(3\pm\rho)$ and the amplitude of the bridging–halogen distortions Δ. Δ is defined as the displacement of the bridging–halogen ion from the midpoint between the neighboring two metal ions. In addition to the choice of M and X, Δ is strongly dependent on the choice of ligands (A) and counter anions (Y) through the H–bonds. The typical complexes which have been investigated so far in detail, have ClO_4^- for the counter anion. By replacing the counter anion from ClO_4^- to halogen ions, the H–bonds between the ligands and the counter anions are strengthened,[11] which induces the decrease of the M–M distance L, and, accordingly, the decrease of the halogen displacement Δ.[3]

Another important effect of the H–bonds to the electronic state manifests itself in the inter–chain interaction. In the mixed–valence Pt or Pd complexes with halogens for the counter anion, a direction of each halogen displacement is two–dimensionally ordered.[3,4] The phases of the halogen distortions within each chain accord with one another in the bc plane, as shown below.

$$\cdot\cdot M^{3-\rho}\cdot\cdot X^{-}-M^{3+\rho}X^{-}\cdot\cdot\cdot M^{3-\rho}\cdot\cdot X^{-}-M^{3+\rho}X^{-}\cdot\cdot\cdot M^{3-\rho}\cdot\cdot X^{-}-M^{3+\rho}X^{-}\cdot\cdot$$
$$\cdot\cdot M^{3-\rho}\cdot\cdot X^{-}-M^{3+\rho}X^{-}\cdot\cdot\cdot M^{3-\rho}\cdot\cdot X^{-}-M^{3+\rho}X^{-}\cdot\cdot\cdot M^{3-\rho}\cdot\cdot X^{-}-M^{3+\rho}X^{-}\cdot\cdot$$
$$\cdot\cdot M^{3-\rho}\cdot\cdot X^{-}-M^{3+\rho}X^{-}\cdot\cdot\cdot M^{3-\rho}\cdot\cdot X^{-}-M^{3+\rho}X^{-}\cdot\cdot\cdot M^{3-\rho}\cdot\cdot X^{-}-M^{3+\rho}X^{-}\cdot\cdot$$

(Figure 1 shows the complex having a 2–D ordering of CDW.) This is not due to the overlapping of the electronic states between the chains but to the interchain coupling through the 2–D tight network of the H–bonds.[3,4,11] So that, although the electronic states are still one–dimensional, a 2–D phase ordering of CDW is formed. However, in the complexes with ClO_4^- for the counter anion, such an ordering is not formed; the H–bond interchain coupling is weak and the crystal seems to be purely one–dimensional. The existence of a 2–D ordering of CDW provides modifications on the photogeneration of the gap states as discussed in the next section.

The lowest excitation of the MX compounds in the CDW states is the CT exciton transition expressed as $(M^{2+}(d^8), M^{4+}(d^6) \rightarrow M^{3+}(d^7), M^{3+}(d^7))$. In Figure 2, the energies of the CT exciton transition (E_{CT}) of the Pt complexes with ethylenediamine and cyclohexanediamine for the ligands are plotted against the distortion parameter d which is defined as 2Δ divided by L. E_{CT} is mainly determined by the energy difference (E_s) between the M^{2+} site and the M^{4+} site. The linear relationship between E_{CT} and d demonstrate the fact that E_s is proportional to d (and Δ).

The $\{Pt(en)_2Br\}(ClO_4)_2$ crystal which has been previously studied is in the monoclinic system

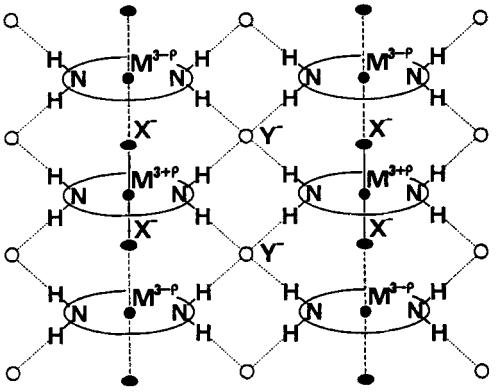

FIGURE 1 Schematic structure of the halogen-bridged metal complex. H-bonds between the amino-groups of the ligands and the counter anions (Y^-) are shown by the dotted lines.

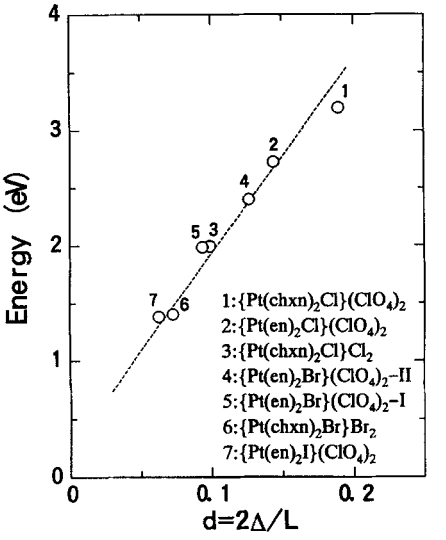

FIGURE 2 The peak energies of the CT absorption bands (E_{CT}) as a function of the distortion parameter d in the Pt complexes.

with the space group $P2_1/a$.[12] This crystal is named $\{Pt(en)_2Br\}(ClO_4)_2$-I in this paper (No.5 in Figure 2). Very recently another polymorphism of this compound named $\{Pt(en)_2Br\}(ClO_4)_2$-II (No.4 in Figure 2) has been discovered,[13] which belongs to the monoclinic system with space group C2/m. In these two complexes, the conformations of the ethylenediamine molecules are slightly different from each other, resulting in the difference of L and Δ (or d).

The important problem is how the relaxation process of the photo-excited state changes by decreasing the bridging-halogen distortions. It has been found that in the complexes with relatively large halogen distortions, the photo-excited state is relaxed to the ground state by radiation of the luminescence with a large stokes shift from the self-trapped exciton state. With decrease of halogen distortions, the exciton luminescence is considerably decreased; e.g. the intensity of luminescence of $\{Pt(en)_2I\}(ClO_4)_2$ is smaller by more than four orders of magnitude than that of $\{Pt(en)_2Cl\}(ClO_4)_2$, while it has been found that the photo-conductivity is enhanced in the complexes having small halogen distortions, e.g. $\{Pt(en)_2I\}(ClO_4)_2$[14] and $\{Pd(chxn)_2Br\}Br_2$[15]. These results suggests that with decrease of the halogen distortions, the radiative decay through the self-trapped exciton state is suppressed and the nonradiative decay including the carrier separation process becomes dominant for the relaxation. From these facts, the complexes having small halogen distortions should be good targets to study the relaxation dynamics of the photo-excited states related to the gap states such as solitons and polarons.

THE PHOTO-INDUCED ABSORPTION STUDIES

The PA spectra of $\{Pt(en)_2Br\}(ClO_4)_2$-I, $\{Pt(en)_2I\}(ClO_4)_2$[16] and $\{Pt(chxn)_2Br\}Br_2$[16] and $\{Pt(chxn)_2I\}I_2$ at 77K are presented in Figure 3. The PA measurements are performed on single crystals for the former three complexes, and on powder samples dispersed in KI pellet for $\{Pt(chxn)_2I\}I_2$, since the thin platelet sample cannot be obtained in $\{Pt(chxn)_2I\}I_2$. The PA spectra in Figure 3 give two types of the spectral features of the PA signals in the MX compounds. In the measurements on single crystals, polarization of both the irradiation light (E_{ex}) and the transmission light (E) is taken parallel to the chain axis b. In Figure 3, the polarized absorption spectra (dotted lines) near the absorption edges at 77K are also presented, which were measured for E//b. The arrows in Figure 3 indicate the peak energies of the CT exciton absorption derived from the Kramars-Kronig transformation of the polarized reflectivity spectra at RT.

The most striking feature of the PA spectra is that in $\{Pt(en)_2Br\}(ClO_4)_2$-I and $\{Pt(en)_2I\}(ClO_4)_2$, the PA signal shows a triplet structure, $\mathbf{a}_1$, $\mathbf{a}_2$ and **b**, while the structure of $\{Pt(chxn)_2Br\}Br_2$ and $\{Pt(chxn)_2I\}I_2$ is a doublet, $\mathbf{a}_1'$ and $\mathbf{a}_2'$; the mid-gap structure **b** located at nearly half of the CT exciton energy, is predominant in $\{Pt(en)_2Br\}(ClO_4)_2$-I and $\{Pt(en)_2I\}(ClO_4)_2$, but it does not exist in $\{Pt(chxn)_2Br\}Br_2$ and $\{Pt(chxn)_2I\}I_2$. In the measurements on the single crystals, the PA signals were characteristic only for E//b and no PA signals could be detected for E⊥b.

In Figure 4 (1-3), the normalized peak-intensities (the photo-induced changes of absorption coefficients $\Delta\alpha$) of the PA structures at 77K are plotted against time in the three single crystal samples. The intensity of the peak **b** decays in a different manner compared with those of the doublet, $\mathbf{a}_1$ and $\mathbf{a}_2$. The components of the doublet, $\mathbf{a}_1$ and $\mathbf{a}_2$ (or $\mathbf{a}_1'$ and $\mathbf{a}_2'$) show the same decay characteristic. Judging from the spectral- and time-characteristics, the optically excited states include two different types of photo-products associated with the doublet and the mid-gap structure **b**.

As discussed in the previous section, the 1-D CDW states of the Pt complexes are characterized by the two parameters, the CT excitation energy E_{CT} and the distortion parameter $d=2\Delta/L$. The relatively small d values, ca. 0.05-0.1, indicate that these complexes belong to the weak or intermediate e-l coupling regime. An important difference among the four complexes exists in the interchain interaction. As mentioned above, the CDW states in $\{Pt(chxn)_2X\}Y_2$ (X,Y=Br,I) are two-dimensionally ordered, while those in $\{Pt(en)_2X\}(ClO_4)_2$ (X=Br,I) are not ordered but purely one-dimensional. Such a change in crystal structure should be reflected in the PA spectra as a result of changes to the 1-D electronic states.

In the 1-D Peierls-Hubbard system, several localized levels associated with the 1-D instability are considered to exist in an intragap region, as schematically illustrated in Figure 5; namely, polarons (P^- or P^+), and spin- and charged-solitons (S^0 and S^- or S^+).[5,6,8] The dynamical properties of these particles are substantially determined by the correlation between the electron-lattice interaction (**S**) and the transfer energy (**T**).[5,6] For the weak coupling case (**S/T**<1), it has been theoretically demonstrated that two absorption bands arise for a polaron and one mid-gap band for either of a spin- or charged-soliton.[5] The transitions due to polarons are indicated by solid

arrows in Figure 5 (1). (The oscillator strengths of the higher transitions indicated by the dashed lines are suggested to be extremely weak.) The mid-gap band due to solitons corresponds to transitions from the valence band (V.B.) to the soliton state or from the soliton state to the con-

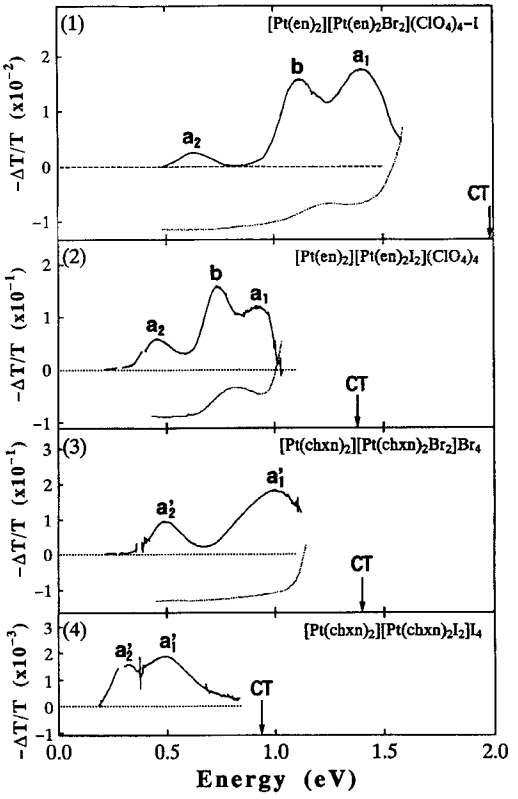

FIGURE 3 The PA spectra $-\Delta T/T$ (solid lines) at 77 K for single crystals of $\{Pt(en)_2Br\}(ClO_4)_2$-I, $\{Pt(en)_2I\}(ClO_4)_2$, $\{Pt(chxn)_2Br\}Br_2$ and powder samples of $\{Pt(chxn)_2I\}I_2$. The excitation light is an Ar laser 5145A (5mW/cm^2 for the single crystal samples and 100mW/cm^2 for the powder samples). In the measurements of the single crystal samples, polarization of both excitation lights (E_{ex}) and transmission lights (E) is parallel to the b axis. The polarized absorption spectra along the b axis of the single crystal samples are also presented by dotted lines in arbitrary units. The arrows indicate the CT exciton energies at RT.

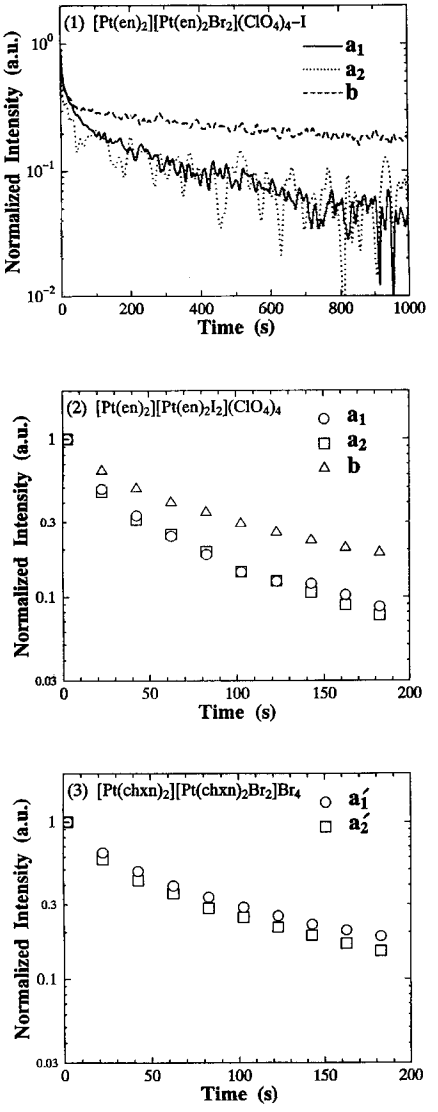

FIGURE 4 Time-dependences of the normalized peak intensities of the structures in the PA spectra (the photo-induced changes of the absorption coefficient $\Delta\alpha$) measured for E_{ex}//b at 77K.

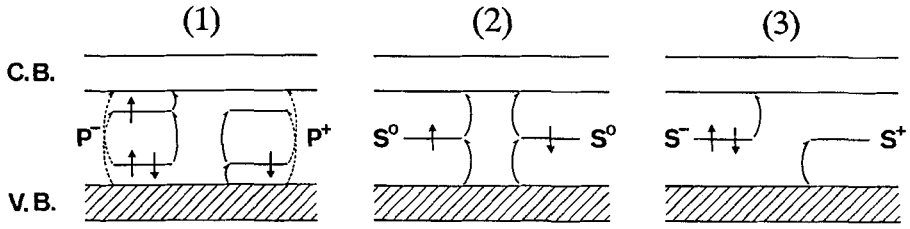

FIGURE 5 Energy level diagrams; (1) polarons (P^-, P^+), (2) spin-solitons (S^0), and (3) charged-solitons (S^-, S^+). Possible optical transitions are indicated by arrows.

duction band (C.B.). The recent calculation based on the two-band model of the Peierls-Hubbard system using reasonable parameters for T, U, and S in the MX compounds, has provided more detailed absorption spectra for the gap states.[7] Comparing the energy positions of the PA bands in Figure 3 with their theoretical predictions, it is natural to assign the doublet to polarons and the **b** band to spin- or charged-solitons.

These assignments are reasonable, taking account of the interchain interaction. Under the 2-D phase ordering of CDW, formation of a dissociated soliton pair requires a large scale of misalignment of CDW phases between the neighboring chains, which leads to excess energy of soliton formation. Accordingly, in the 2-D ordered complex, $\{Pt(chxn)_2X\}Y_2$ (X,Y=Br,I), soliton formation would be suppressed. On the other hand, a polaron pair does not produce such misalignment of CDW phases, so that polarons are produced even in $\{Pt(chxn)_2X\}Y_2$ (X,Y=Br,I).

As seen in Figure 4, the decay time of the PA signals decreases with decrease of d. In fact, the PA signals of $\{Pt(chxn)_2I\}I_2$ have been found to decay completely at least within 10 seconds at 77K. Such a tendency suggests that with decrease of d, the mobility of the gap states increases due to decrease of the polaronic effects, that is, to delocarization of the electronic states.

To obtain further information about the relaxation process of the photo-excited states, we measured the excitation profiles of the PA bands on $\{Pt(en)_2Br\}(ClO_4)_2$-I and $\{Pt(en)_2I\}(ClO_4)_2$, which are plotted in Figure 6. As seen, the CT exciton does not contribute to generation of solitons and polarons in both complexes. This is considered mainly due to the excitonic effect on the photo-excited electron-hole pairs which is induced by the nearest neighbor Coulomb interaction V. Within the scheme of the adiabatic potential model, there exists a potential barrier between the CT exciton and the local minimum of soliton or polaron states. In fact, the excitation energy dependence of the PA signals in $\{Pt(en)_2I\}(ClO_4)_2$ is almost the same as that of the photoconductivities along the b axis reported by Haruki et al.,[14] suggesting that a free electron-hole pair is able to contribute to the formation of charged-particles, that is, polarons and/or charged-solitons. In this relaxation channel, spin-solitons are negligible, since they have no charges.

In the above discussion, however, it is difficult to confirm whether the photo-generation of spin-solitons can be neglected in any relaxation processes. In the ESR measurements on as-grown samples of $\{Pt(en)_2I\}(ClO_4)_2$ and $\{Pt(en)_2Br\}(ClO_4)_2$-I, a finite amount of paramagnetic spins (ca. 10^{-4} per site) were detected.[17] In our previous papers,[4,18] they have been attributed to

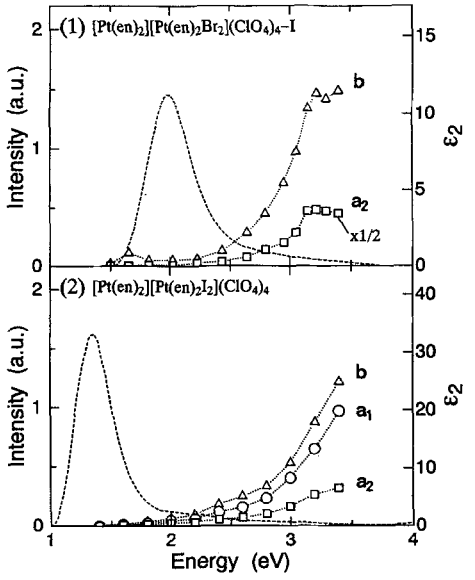

FIGURE 6 The excitation spectra for the peak intensities of the PA bands at 77K with E_{ex}//b and the imaginary parts of the dielectric constants ε_2 at RT (broken lines) in $\{Pt(en)_2Br\}(ClO_4)_2$-I and $\{Pt(en)_2I\}(ClO_4)_2$.

spin-solitons confined by some crystal imperfections. Corresponding to these defects, a weak absorption band was observed at nearly half of the gap energies in these two complexes as shown by the dotted lines in the upper part of Figure 3. However, in the 2-D ordered MX compounds, $\{Pt(chxn)_2Br\}Br_2$, neither such a defect-related absorption band nor paramagnetic spin has been detected.[4,18] Accordingly, taking account of the energy difference between the defect-induced absorption band and the **b** band, the **b** band is attributable to charged-solitons.

The absorption for the gap states of the MX compounds previously reported are mostly related to $\{Pt(en)_2Cl\}(ClO_4)_2$.[9,19-21] Since this complex is in the strong e-l coupling regime characterized by a large **S/T**, our results in the domain of the small **S/T** can not be directly compared with their data. In fact, the spectral features of the PA signals presented in Figure 3 are quite different from those of $\{Pt(en)_2Cl\}(ClO_4)_2$.[9,19] In Figure 7, the PA spectrum of $\{Pt(en)_2Br\}(ClO_4)_2$-II which has been newly synthesized, is presented together with the result of $\{Pt(en)_2Cl\}(ClO_4)_2$. The polarized absorption spectra near the band edge are also shown by the dotted lines. As seen, the features of the PA spectra of the two complexes are very similar to each other; there exists two weak absorption bands **A** and **B** just below the band edge in as-grown samples and they are enhanced by light irradiations. Figure 8 shows the excitation profiles of the **A** bands in these two complexes at 77K. In $\{Pt(en)_2Cl\}(ClO_4)_2$, the PA bands do not decay at this temperature so that the PA measurements at each excitation energy were performed with extremely low excitation powers. The results of $\{Pt(en)_2Cl\}(ClO_4)_2$ is qualitatively in agreement with that previously reported.[21] In $\{Pt(en)_2Br\}(ClO_4)_2$-II, the PA bands are not stable but their life time is very long at 77K, which is estimated about 20 minutes when assuming the exponential decay. The long life time of PA signals in these complexes suggests the formation of localized defect-like states.

The most important feature of Figure 8 is that the **A** bands of both complexes can be generated

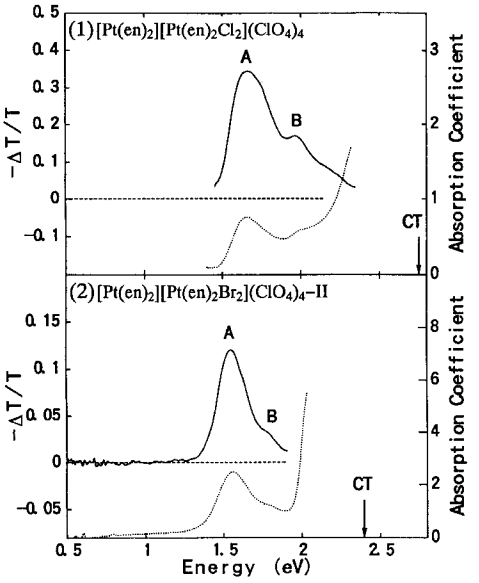

FIGURE 7 The PA spectra for the excitation lights of 5145A (E_{ex}//b) (solid lines) and the polarized absorption spectra (dotted lines) of $\{Pt(en)_2Cl\}(ClO_4)_2$ and $\{Pt(en)_2Br\}(ClO_4)_2$-II at 77K. The arrows indicate the CT exciton energies.

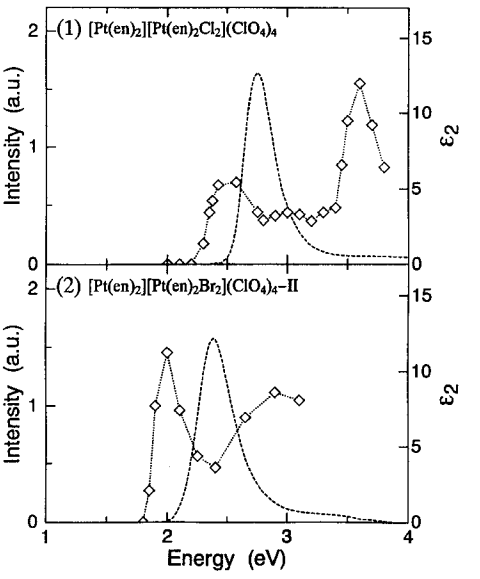

FIGURE 8 The excitation profiles (squares) of the PA bands **A** with E_{ex}//b at 77K in $\{Pt(en)_2Cl\}(ClO_4)_2$ and $\{Pt(en)_2Br\}(ClO_4)_2$-II. The broken lines show ε_2. ε_2 of $\{Pt(en)_2Cl\}(ClO_4)_2$ has been taken from Ref.21 reported by Wada et al..

by irradiation of lights with the energies nearly equal to or even lower than the CT exciton energies. This is essentially different from the results of $\{Pt(en)_2I\}(ClO_4)_2$ and $\{Pt(en)_2Br\}(ClO_4)_2$-I having the small halogen distortions in Figure 6. Such a difference in the two types of complexes cannot be attributed to the difference in the crystal structures including the conformations of ligand molecules mentioned above, since $\{Pt(en)_2Cl\}(ClO_4)_2$ and $\{Pt(en)_2Br\}(ClO_4)_2$-I belong to the same space group, $P2_1/a$, and $\{Pt(en)_2Br\}(ClO_4)_2$-II and $\{Pt(en)_2I\}(ClO_4)_2$ to C2/m. Therefore, the obtained results of the PA measurements suggest that the **A** (and **B**) bands have the different origin from those of the $\mathbf{a}_1$, $\mathbf{a}_2$ and **b** bands, that is, polaron or charged-solitons. In $\{Pt(en)_2Cl\}(ClO_4)_2$, both the excitonic effect (**V/T**) and the e-l interaction (**S/T**) should be larger than those in $\{Pt(en)_2I\}(ClO_4)_2$. So that, it is expected that the carrier separation from the CT exciton is more difficult to occur in $\{Pt(en)_2Cl\}(ClO_4)_2$, as compared with $\{Pt(en)_2I\}(ClO_4)_2$. An important information about the origin of the **A** and **B** bands in $\{Pt(en)_2Cl\}(ClO_4)_2$ has been given by the photo-induced ESR measurements.[22,23] According to them, the excited states responsible for the **A** and **B** bands have spin s=1/2. Considering these PA and ESR measurements, the **A** and **B** bands might be attributed to spin-soliton-like defect states. There remains, however, several unsolvable experimental results, some of which support the polarons as the

origin of the **A** and **B** bands.[9,20,22] More detail experiments seem to be necessary to determine precisely the origin of the **A** and **B** bands. A most important point at the present stage is that the features of the photo-induced gap states are strongly dependent on the magnitude of **S/T**.

Finally, we emphasize again that photogenerations of the gap states in MX chains strongly depend on the two factors: (1) the interchain interaction of CDW and (2) the effective magnitude of the e-l interaction **S/T** (or the amplitude of CDW). As for the interchain interaction, small interchain coupling ensures 1-D character of CDW and leads to an appearance of the mid-gap band, which is regarded as evidence for soliton formation. On the other hand, the PA structures assigned to polarons are insensitive to the dimensionality of CDW. Concerning the e-l interactions, delocalization of the electronic states due to decrease of **S/T** leads to increase of efficiency of the photo-induced carrier separations and to decrease of life time of the gap states, while localization effects on the excitons or electrons and holes due to increase of **S/T** (and simultaneously increase of **V/T**) seem to change remarkably the generation process and the stabilization energy of each gap state. Such various behaviors of the gap states in MX chains present an important problem valuable for understanding of the nonlinear excitations in the 1-D electronic systems.

We are grateful to Prof. K. Nasu and Dr. Iwano (KEK) for many enlightening discussions.

REFERENCES

1. W.P. Su, J.R. Schrieffer, and A.J. Heeger, Phys. Rev. Lett., 42, 1698 (1979), and Phys. Rev., B22, 2099 (1980).
2. For a review, see A.J. Heeger, S. Kivelson, and J. R. Schrieffer, Rev. Mod. Phys., 60, 781 (1988).
3. H. Okamoto, T. Mitani, K. Toriumi, and M. Yamashita, Mater. Sci. Eng., 13, L9 (1992).
4. H. Okamoto, K. Toriumi, T. Mitani, and M. Yamashita, Phys. Rev., B42, 10381 (1990).
5. Y. Tagawa and N. Suzuki, J. Phys. Soc. Jpn., 59, 4074 (1990).
6. J.T. Gammel, A. Saxena, I. Batistic, A.R. Bishop, and S.R. Phillpot, Phys. Rev., B45, 6408 (1992).
7. S.M. Weber-Milbrodt, J.T. Gammel, A.R. Bishop, and E.Y. Loh,Jr., Phys. Rev., B45, 6435 (1992).
8. K. Iwano and K. Nasu, J. Phys. Soc. Jpn., 61, 1380 (1992).
9. S. Kurita, M. Haruki, and K. Miyagawa, J. Phys. Soc. Jpn., 57, 1789 (1988).
10. H. Okamoto, K. Okaniwa, T. Mitani, K. Toriumi, and M. Yamashita, Solid State Commun, 77, 465 (1991).
11. K. Okaniwa, H. Okamoto, T. Mitani, K. Toriumi, and M. Yamashita, J. Phys. Soc. Jpn., 60, 997 (1991).
12. K. Toriumi, M. Yamashita, S. Kurita, I. Murase, and T. Ito, Acta Cryst., B49, 497 (1993).
13. H. Okamoto et al., unpublished.
14. M. Haruki, M. Tanaka, and S. Kurita, Synth. Met., 19, 901 (1987).
15. H. Okamoto et al., unpublished.
16. H. Okamoto, T. Mitani, K. Toriumi, and M. Yamashita, Phys. Rev. Lett., 69, 2248 (1992).
17. A. Kawamori, R. Aoki, and M. Yamashita, J. Phys., C18, 5487 (1985).
18. H. Okamoto, K. Toriumi, T. Mitani, and M. Yamashita, Mol. Cryst. Liq. Cryst., 218, 247 (1992).
19. N. Kuroda, M. Sakai, Y. Nishina, M. Tanaka, and S. Kurita, Phys. Rev. Lett., 58, 2122 (1987).
20. R.J. Donohoe, S.A. Ekberg, C.D. Tait, and B.I. Swanson, Solid State Commun., 71, 49 (1989).
21. Y. Wada, N. Matsushita, and M. Yamashita, Mol. Cryst. Liq. Cryst., 216, 175 (1992).
22. S. Kurita and M. Haruki, Synth. Met., 29, F129 (1989).
23. N. Kuroda, M. Sakai, M. Suezawa, Y. Nishina, and K. Sumino, J. Phys. Soc. Jpn., 59, 3049 (1990).